

# A Study in Dataset Pruning for Image Super-Resolution

Brian B. Moser<sup>1,2</sup>[0000–0002–0290–7904], Federico Raue<sup>1</sup>[0000–0002–8604–6207], and  
Andreas Dengel<sup>1,2</sup>[0000–0002–6100–8255]

<sup>1</sup> German Research Center for Artificial Intelligence (DFKI), Germany

<sup>2</sup> RPTU Kaiserslautern-Landau, Germany

first.second@dfki.de

**Abstract.** In image Super-Resolution (SR), relying on large datasets for training is a double-edged sword. While offering rich training material, they also demand substantial computational and storage resources. In this work, we analyze dataset pruning as a solution to these challenges. We introduce a novel approach that reduces a dataset to a core-set of training samples, selected based on their loss values as determined by a simple pre-trained SR model. By focusing the training on just 50% of the original dataset, specifically on the samples characterized by the highest loss values, we achieve results comparable to or even surpassing those obtained from training on the entire dataset. Interestingly, our analysis reveals that the top 5% of samples with the highest loss values negatively affect the training process. Excluding these samples and adjusting the selection to favor easier samples further enhances training outcomes. Our work opens new perspectives to the untapped potential of dataset pruning in image SR. It suggests that careful selection of training data based on loss-value metrics can lead to better SR models, challenging the conventional wisdom that more data inevitably leads to better performance.

**Keywords:** Super-Resolution · Dataset Pruning · Core-Set Selection.

## 1 Introduction

Image Super-Resolution (SR) techniques are a cornerstone of image processing as they reconstruct High-Resolution (HR) images from their Low-Resolution (LR) counterparts [30,26,27,11]. It has wide-ranging applications, from enhancing consumer photography to improving satellite or medical imagery [28,24,3,37]. Despite its relevance, training SR models requires substantial computational resources due to large-scale datasets [13,24]. These datasets are pivotal for capturing the diversity of textures and patterns essential for effective upscaling, but they also pose significant storage challenges [19]. Recent advancements in deep learning have propelled SR techniques to new heights, with models like SwinIR or HAT taking the lead by setting new benchmarks for regression-based image enhancement quality [18,7].

However, the success of these models often hinges on their capacity to learn from extensive and diverse training data, exacerbating the resource-intensive nature of SR model training [28,24]. In response to these challenges, our work explores dataset pruning as a strategy to enhance the efficiency of SR model training without compromising the quality of the output images [1,33,8]. To the best of our knowledge, efforts to apply dataset pruning to image SR tasks have been scarce, except for the notable contribution made by *Ding et al.* [10], which we will discuss and improve on in this work. The concept of dataset pruning involves reducing the size of the training dataset by selectively identifying a subset of samples that are most informative for the optimization process. This approach is promising for mitigating the storage burden of large datasets while preserving or improving the training performance of SR models [13,25].

Our contribution is twofold. First, we propose a novel loss-value-based sampling method for dataset pruning in image SR, leveraging a simple pre-trained SR model, namely SRCNN [11]. Our method contrasts traditional approaches that indiscriminately use the entirety of available data, i.e., DIV2K [2]. Secondly, we empirically demonstrate that training SR models on a pruned dataset - comprising 50% of the original dataset selected based on their loss values - can achieve comparable or superior performance to training on the full dataset. Refining this selection by excluding the top 5% hardest samples, which we found were counterproductive, further enhances model training efficiency.

Through this work, we aim to spark a paradigm shift in how training datasets are curated for SR tasks. We advocate for a loss-value-driven approach to dataset pruning. Our strategy significantly reduces the storage requirements of SR model training and offers a scalable solution that can adapt to the evolving complexities and requirements of image SR.

## 2 Related Work

Dataset pruning is particularly interesting to deep learning [1,33,8]. It focuses on training set size reduction while attempting to maintain or even enhance the performance of models. This process is not just about economizing on computational storage; it also aims to improve model generalization by eliminating redundant or less informative samples [17,14]. Various methodologies have explored this concept, including importance sampling, core-set selection, and data distillation. In the following, we explore key contributions to dataset pruning and provide insights into its development.

**Importance Sampling.** One key approach in dataset pruning is importance sampling, where the idea is to prioritize training on samples that are deemed more important for the model. Works such as *Katharopoulos et al.* [17] have explored adaptive sampling methods that dynamically adjust the probability of selecting each sample based on the model’s current state. These methods aim to focus computational effort where it is most needed. However, by weighting samples, importance sampling does not reduce the training set size as we do.

**Data distillation.** Data distillation is a technique that generates a condensed and synthetic version of the training data, often through knowledge distillation [14], where a smaller dataset is created to capture the essence of the original data. The work by *Wang et al.* [38] on dataset distillation demonstrates how training on a distilled dataset can achieve comparable performance to training on the entire dataset, significantly reducing the computational burden regarding convergence and storage. Since then, various exciting developments have been made in dataset distillation [29,6]. Nevertheless, existing approaches to dataset distillation are predominantly aimed at capturing critical semantic details for image classification purposes [42,5,31,43]. Given the significant differences that exist between image classification and image SR, applying dataset distillation techniques directly to SR tasks presents a considerable challenge [19].

**Core-Set Selection.** This approach involves identifying a subset of the training data that is a good representation of the entire dataset. Therefore, it reduces the dataset size in contrast to importance sampling. *Sener et al.* [34] introduced an optimization framework that selects samples constituting a core-set for training deep neural networks. This method is grounded in the principle of minimizing the maximum loss over the dataset, ensuring the selected subset is as informative as the full original dataset. Since then, core-set selection, also called proxy datasets, has been further developed in various fields, such as image classification or neural architecture search [25,10,8,35].

To the best of our knowledge, image SR tasks have primarily remained untouched by initiatives in dataset pruning, with a notable exception of the work conducted by *Ding et al.* [10]. The authors suggest using the Sobel filter to reduce the dataset, focusing specifically on selecting samples with rich textures. They further refine their selection by clustering these texture-rich samples to ensure a variety of textures is represented. In contrast, we opt for sampling based on SR reconstruction loss values. In the experiments section, we will demonstrate that our strategy, which prioritizes samples according to their SR reconstruction loss, performs better than a method based on Sobel filter selection.

### 3 Methodology

In this section, we introduce our method for optimizing SR model training through dataset pruning. Our approach is found on the premise that not all samples in a dataset contribute equally to the learning process in the context of SR tasks [34,17,25]. By carefully selecting a core-set of samples that are most informative for SR model training, we aim to enhance the learning process.

After introducing the concept of core-sets and how they are sampled, we present our loss-based sampling method, which leverages a pre-trained SR model - a simple SRCNN [11] - to estimate the complexity in reconstructing HR samples from their LR counterparts. By focusing on challenging samples for the SR model, as indicated by higher loss values, we hypothesize that the model can learn more effectively, thereby improving its performance on unseen data.

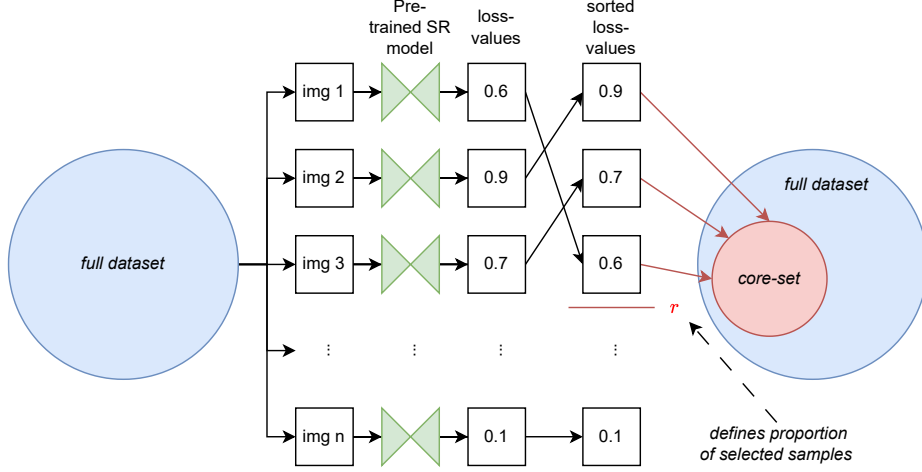


**Fig. 1.** Illustration of our loss-value-based core-set selection for image SR. Initially, the full dataset undergoes evaluation through a pre-trained SR model to calculate loss values for each image pair. These loss values are then sorted to identify samples with varying degrees of reconstruction difficulty. A pre-defined proportion  $r$  of these samples is selected to form a core-set.

### 3.1 Core-Sets

Consider a dataset  $\mathcal{D} = \{(\mathbf{x}_i, \mathbf{y}_i)\}$  with a total number of elements denoted as  $N_{\mathcal{D}}$ . In this context,  $\mathbf{x}_i$ , where  $0 \leq i < N_{\mathcal{D}}$ , represents the  $i$ -th LR sample and  $\mathbf{y}_i$  its corresponding HR counterpart. We define a subset of  $\mathcal{D}$ , denoted by  $\mathcal{D}_r \subset \mathcal{D}$ , as a core-set with a size of  $N_{\mathcal{D}_r}$ . The proportion  $r \in (0, 1)$  specifies the size of  $\mathcal{D}_r$  relative to  $\mathcal{D}$ :  $N_{\mathcal{D}_r} \approx r \cdot N_{\mathcal{D}}$ . This approximation accounts for instances where the dataset size cannot be divided evenly. The core-set acts between the original dataset and the SR model to enhance the SR output quality by focusing on important samples during training. The objective is to construct a core-set  $\mathcal{D}_r \subset \mathcal{D}$  such that its size  $N_{\mathcal{D}_r} \approx r \cdot N_{\mathcal{D}}$ , with  $r \in (0, 1)$ . To achieve this for any chosen  $r$ , the sampling strategy must satisfy the condition

$$N_{\mathcal{D}_r} = \sum_{(\mathbf{x}_i, \mathbf{y}_i) \in \mathcal{D}} \mathbb{1}_{\mathcal{D}_r}(\mathbf{x}_i) \approx r \cdot N_{\mathcal{D}}, \quad (1)$$

where  $\mathbb{1}_{\mathcal{D}_r} : \mathcal{D} \rightarrow \{0, 1\}$  is the indicator that determines whether an element belongs to the core-set  $\mathcal{D}_r$  within the larger dataset  $\mathcal{D}$ .

The concrete realization of the core-set selection depends on the sampling mechanism. *Ding et al.* [10] proposed to use the Sobel filter to identify texture-rich training samples. In contrast, we argue that a loss-value-based sampling is more efficient, which we will explain next and demonstrate empirically in the experiments section.

### 3.2 Loss-Value-based Sampling

In image SR, one approximates  $\mathbf{y}_i \approx \mathcal{M}(d(\mathbf{y}_i))$  with a SR model  $\mathcal{M}$  and a degradation function  $d$  that represents the relationship between the HR and LR space (i.e.,  $d(\mathbf{y}_i) = \mathbf{x}_i$ ). As a result, a trained SR model can provide a distance metric based on a loss function. Let  $\mathcal{L} : \mathbb{R}^{h \times w \times c} \times \mathbb{R}^{h \times w \times c} \rightarrow \mathbb{R}$  be a loss function, e.g., Mean Squared Error (MSE), with  $h, w, c$  as the height, width, and channel size, respectively. Given  $r \in (0, 1)$ , we can derive a core-set with

$$\mathcal{D}_r^{\text{ASC}} = \arg \min_{\substack{\mathcal{D}' \subset \mathcal{D}, \\ \text{s.t. } |\mathcal{D}'| \approx r \cdot N_{\mathcal{D}}}} \sum_{(\cdot, \mathbf{y}_i) \in \mathcal{D}'} \mathcal{L}(\mathcal{M}(d(\mathbf{y}_i)), \mathbf{y}_i), \quad (2)$$

where samples with high loss values are removed, denoted as ascending sampling (ASC). Likewise, we can define a sampling method based on removing the lowest loss values, thereby concentrating on hard samples, by

$$\mathcal{D}_r^{\text{DES}} = \arg \max_{\substack{\mathcal{D}' \subset \mathcal{D}, \\ \text{s.t. } |\mathcal{D}'| \approx r \cdot N_{\mathcal{D}}}} \sum_{(\cdot, \mathbf{y}_i) \in \mathcal{D}'} \mathcal{L}(\mathcal{M}(d(\mathbf{y}_i)), \mathbf{y}_i), \quad (3)$$

denoted as descending sampling (DES). The concept is illustrated in Figure 1. In the experiments section, we will determine whether to favor ascending or descending sampling and which  $r$  value is beneficial. Intuitively, ascending sampling includes less complex, monochromatic training samples first, whereas descending sampling favors texture-rich, multi-colored training samplings. In the following, we will use a simple pre-trained SRCNN [11] (composed of three layers of convolutions) and MSE for the loss calculation in Equation 2 and Equation 3.

## 4 Experiments

In this section, we empirically evaluate the performance of our loss-value-based sampling. We start by benchmarking whether ascending (ASC) or descending (DES) sampling is more beneficial. We also evaluate whether maintaining the same number of training steps is critical. Next, we compare our loss-value-based sampling with the sampling mechanism exchanged by using Sobel filters instead, as suggested by *Ding et al.* [10]. Finally, we analyze the pruned dataset and suggest a refined version. We will evaluate the original and refined core-set with state-of-the-art datasets and methods.

### 4.1 Datasets

Our method is assessed using well-established SR datasets. The DIV2K dataset [2] served as our primary source for training data, from which we extracted sub-images according to standard practice in literature [3,30]. As a result, we derive around 32K HR training samples from 800 2K HR images. LR samples are computed by following the standard procedure using bicubic interpolation

and anti-aliasing [21,28]. These sub-images formed the basis for selecting the core-sets. For the evaluation phase, we utilized the test datasets Set5 [4], Set14 [39], BSDS100 [20], and Urban100 [15]. We assess our experiments based on two metrics: Peak Signal-to-Noise Ratio (PSNR) and Structural Similarity Index (SSIM), where higher values represent better image quality.

## 4.2 Results

**Table 1.** Comparison of ascending and descending sampling on BSD100 with  $2\times$  scaling. Values with at least the same or better performance than their corresponding performance on the full dataset are highlighted in **red**.

Method	Train Steps	FSRCNN [12]		DRRN [36]		IDN [16]		RDN [41]		SwinIR [18]	
		PSNR	SSIM	PSNR	SSIM	PSNR	SSIM	PSNR	SSIM	PSNR	SSIM
full	15,608	31.09	0.8955	29.42	0.8781	31.98	0.9076	32.25	0.9103	32.23	0.9103
75% ASC	11,706	30.84	0.8928	28.11	0.8725	31.90	0.9065	32.21	0.9101	32.13	0.9091
50% ASC	7,804	30.25	0.8862	22.28	0.8370	31.67	0.9040	32.02	0.9080	31.90	0.9067
25% ASC	3,902	28.38	0.8303	14.66	0.7293	31.23	0.8976	31.66	0.9039	30.97	0.8957
75% DES	11,706	<b>31.11</b>	<b>0.8960</b>	29.32	<b>0.8783</b>	31.96	0.9071	<b>32.26</b>	<b>0.9107</b>	<b>32.24</b>	<b>0.9104</b>
50% DES	7,804	<b>31.20</b>	<b>0.8968</b>	29.40	<b>0.8795</b>	31.94	0.9070	<b>32.25</b>	<b>0.9105</b>	32.21	0.9101
25% DES	3,902	30.98	0.8937	29.32	<b>0.8791</b>	31.81	0.9052	32.22	0.9099	32.13	0.9088
25% DES	7,804	<b>31.11</b>	<b>0.8969</b>	29.39	<b>0.8804</b>	31.94	0.9068	32.24	<b>0.9104</b>	32.20	0.9096
25% DES	15,608	<b>31.35</b>	<b>0.8986</b>	<b>29.46</b>	<b>0.8810</b>	31.98	<b>0.9076</b>	<b>32.26</b>	<b>0.9104</b>	<b>32.24</b>	0.9101
50% DES	15,608	<b>31.30</b>	<b>0.8983</b>	29.39	<b>0.8795</b>	<b>32.00</b>	<b>0.9076</b>	<b>32.28</b>	<b>0.9108</b>	<b>32.27</b>	<b>0.9104</b>

**Ascending versus Descending Sampling.** We compare ascending (ASC) and descending (DES) sampling methods on the BSD100 dataset with  $2\times$  scaling in Table 1. Our primary focus is understanding their impact on various image SR models, namely FSRCNN [12], DRRN [36], IDN [16], RDN [41], and SwinIR [18]. The various models are used to evaluate different categories of SR models, namely simple CNN, recursive CNN, residual CNNs, and Transformer-based [28].

We observe a general trend of declining performance, i.e., worse image enhancement quality, across all models when ascending sampling (ASC) is applied at reduced dataset sizes. Specifically, at 25% dataset size, the performance drop becomes more pronounced, with the PSNR dropping from 31.09 to 28.38 for FSRCNN and from 29.42 to 14.66 for DRRN. This indicates the ineffectiveness of ascending sampling in preserving model performance.

In contrast, descending sampling generally outperforms or matches the full dataset performance, especially notable in the 75% and 50% dataset sizes. For instance, FSRCNN shows improved results at 75% DES and even higher scores at 50% DES, surpassing the full dataset baseline.

Note that decreased data size leads to fewer training steps if the number of epochs is fixed. Consequently, with fixed epochs, i.e., 200, SR models train



**Fig. 2.** Comparison of top-selected samples by ascending and descending sampling. We can observe that descending sampling selects primarily training patches with high textural details, whereas ascending sampling focuses on monochromatic samples.

**Table 2.** Quantitative comparison between sampling based on loss-value and Sobel filter (average PSNR/SSIM) with SwinIR for classical image SR on benchmark datasets ( $2\times$  scaling, 50% pruning). The best performance is highlighted in red.

Sampling Method	Set5 [4]		Set14 [39]		BSD100 [20]		Urban100 [15]		Manga109 [22]	
	PSNR	SSIM	PSNR	SSIM	PSNR	SSIM	PSNR	SSIM	PSNR	SSIM
loss-based	38.32	0.9619	34.15	0.9232	32.45	0.9038	33.43	0.9396	39.55	0.9790
sobel-based	38.26	0.9612	34.09	0.9225	32.44	0.9037	33.38	0.9392	39.54	0.9789

effectively shorter because a single epoch has fewer training iterations due to the reduced data size. Remarkably, applying more epochs to match the number of training steps on the original dataset further enhances the results. Using 25% DES with 4x epochs, which is equal to the number of training steps employed in the full dataset, achieves the highest PSNR and SSIM for several models.

Our findings highlight that hard samples, defined by high loss, are crucial for maintaining or enhancing SR model performance. Therefore, texture-rich samples, contrary to monochromatic easy samples (see Figure 2), are significant for training a SR model effectively. Additionally, maintaining the number of training iterations is essential, rather than merely focusing on reducing the dataset size for reduced training time. By keeping training iterations consistent, descending sampling effectively leverages a reduced but more potent subset of the original dataset, leading to improved or comparable performance across all evaluated SR models. Our findings about keeping the same training iterations present a distinct divergence from those reported by Ding et al. [10]. We speculate that this discrepancy may arise from their utilization of fewer training epochs, which likely prevented their models from achieving full convergence. Moving forward, we will further explore our loss-based sampling approach by maintaining a consistent number of iterations and employing the descending sampling technique.

**Loss-based versus Sobel-based** As introduced by Ding et al. [10], utilizing the Sobel filter represents another strategy for curating a core-set for image SR. Therefore, we compare our loss-based sampling method with the Sobel filter approach. From Table 2, it is evident that the loss-based sampling method con-

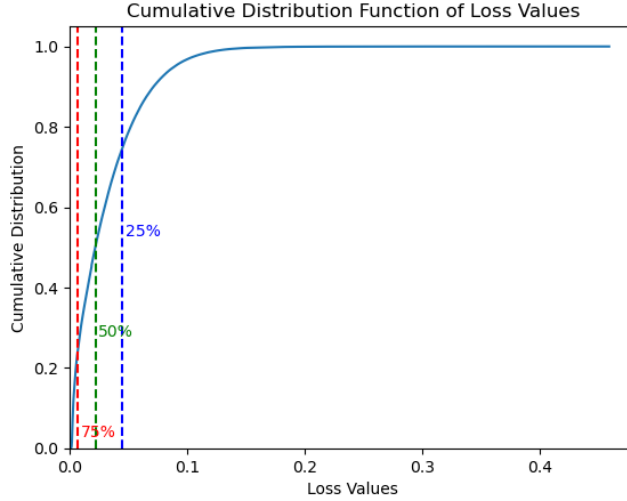


**Fig. 3.** Cumulative Loss-Value Distribution (sorted). Vertical lines represent different descending sampling endpoints for 25%, 50%, and 75% sampling. The right side of the respective vertical line shows the loss values included and found within the corresponding core-sets.

sistently outperforms the Sobel filter-based approach across all datasets. Specifically, for the Set5 dataset, loss-based sampling achieves a PSNR of 38.32 and an SSIM of 0.9619, compared to 38.26 (PSNR) and 0.9612 (SSIM) for the Sobel-based method. This trend continues across the Set14, BSD100, and Urban100 datasets, where loss-based sampling performs superiorly in both PSNR and SSIM metrics. By focusing on loss-values, we prioritize samples the model finds challenging to reconstruct, potentially leading to a more robust learning process and improved SR performance. In contrast, the Sobel filter-based approach, which selects samples based on texture richness, might overlook other crucial aspects contributing to the overall quality and effectiveness of SR reconstruction.

**Analyzing Loss Values.** In this section, we examine the core-sets derived by descending sampling more closely. More specifically, we derive the loss values that can be found by applying descending sampling at 25%, 50%, and 75%. Figure 3 shows the result. The distribution demonstrates that certain samples, characterized by notably higher loss values, are consistently included across all core-sets (see the long tail on the right side of the vertical lines). We theorize that these samples, possibly due to their high noise levels, could be detrimental to the training of SR models. To address this, we suggest refining the initially derived core-set by adjusting the selection threshold by 5% to favor samples with lower loss values and exclude those with the highest losses.

The modified core-set and associated loss values within this refined set are depicted in Figure 4; see the area between the vertical lines denoted by start



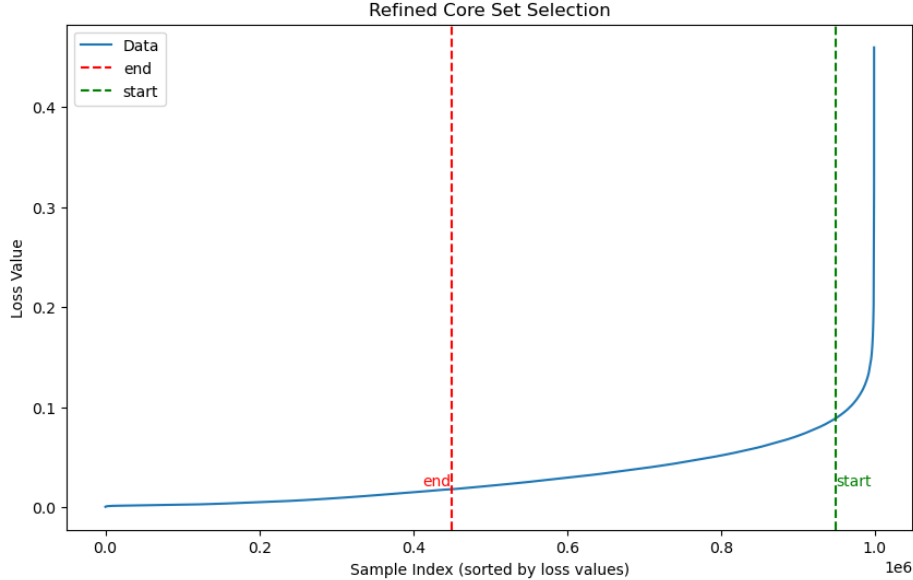


**Fig. 4.** Refined Core Set Proposal. This strategy selects the top 50% most challenging samples but modifies the selection by shifting the inclusion threshold by 5 % towards samples with lower loss values, aiming for a more balanced core-set. In other words, we keep 50 % of the hardest samples in our core-set after excluding the top 5 % from the dataset.

and end. This approach involves retaining 50% of the samples that are initially considered the most challenging but adjusting the selection to slightly favor easier samples (those with lower loss values) by shifting the inclusion criteria by 5%. To put it in another way, the core-set still contains 50% of the hardest samples of the original dataset, except the top 5% hardest. We will evaluate both core-sets, the original and the refined, in the following with state-of-the-art benchmarks.

**Benchmark with State-of-the-Art.** We evaluate the quality of our core-sets by training the state-of-the-art SR model SwinIR [18] on them. The evaluation includes other state-of-the-art methods for classical image SR across benchmark datasets, including Set5 [4], Set14 [39], BSD100 [20], and Urban100 [15], with scaling factors of  $2\times$ ,  $3\times$ , and  $4\times$ . Table 3 reports the results with notable performances being color-coded, with the best and second-best results marked in red and blue, respectively.

Interestingly, when SwinIR is trained on 50% of the dataset for  $2\times$  scaling, it maintains its superior performance on Set5 and improves upon the full dataset results on Set14, BSD100, and Urban100, suggesting efficient learning from a pruned dataset. The refined 50% core-set further improves performance, pushing

**Table 3.** Quantitative comparison (average PSNR/SSIM) with state-of-the-art methods for classical image SR on benchmark datasets (Set5, Set14, BSDS100, and Urban100). These experiments were evaluated under the lense of various scaling factors, specifically 2, 3, and 4. We trained SwinIR on our pruned datasets with 50 % of the size of the original datasets. Moreover, we included our refined version of our core-set, which excludes the top 5% hardest samples (see ref. 50 %). The best and second best performances are in red and blue colors, respectively. As a result, training SwinIR on half of the original datasets leads to comparable and, in most cases, superior performance.

Method	Scale	Train Set	Set5 [4]		Set14 [39]		BSD100 [20]		Urban100 [15]	
			PSNR	SSIM	PSNR	SSIM	PSNR	SSIM	PSNR	SSIM
RCAN [40]	×2	full	38.27	0.9614	34.12	0.9216	32.41	0.9027	33.34	0.9384
SAN [9]	×2	full	38.31	0.9620	34.07	0.9213	32.42	0.9028	33.10	0.9370
IGNN [44]	×2	full	38.24	0.9613	34.07	0.9217	32.41	0.9025	33.23	0.9383
HAN [32]	×2	full	38.27	0.9614	34.16	0.9217	32.41	0.9027	33.35	0.9385
NLSA [23]	×2	full	38.34	0.9618	34.08	0.9231	32.43	0.9027	33.42	0.9394
<b>SwinIR</b> [18]	×2	full	38.35	0.9620	34.14	0.9227	32.44	0.9030	33.40	0.9393
<b>SwinIR</b> [18]	×2	50%	38.35	0.9620	34.20	0.9230	32.46	0.9039	33.47	0.9399
<b>SwinIR</b> [18]	×2	ref. 50%	38.34	0.9619	34.23	0.9236	32.48	0.9041	33.52	0.9401
RCAN [40]	×3	full	34.74	0.9299	30.65	0.8482	29.32	0.8111	29.09	0.8702
SAN [9]	×3	full	34.75	0.9300	30.59	0.8476	29.33	0.8112	28.93	0.8671
IGNN [44]	×3	full	34.72	0.9298	30.66	0.8484	29.31	0.8105	29.03	0.8696
HAN [32]	×3	full	34.75	0.9299	30.67	0.8483	29.32	0.8110	29.10	0.8705
NLSA [23]	×3	full	34.85	0.9306	30.70	0.8485	29.34	0.8117	29.25	0.8726
<b>SwinIR</b> [18]	×3	full	34.89	0.9312	30.77	0.8503	29.37	0.8124	29.29	0.8744
<b>SwinIR</b> [18]	×3	50%	34.87	0.9307	30.70	0.8503	29.35	0.8134	29.19	0.8731
<b>SwinIR</b> [18]	×3	ref. 50%	34.84	0.9306	30.75	0.8506	29.37	0.8137	29.25	0.8740
RCAN [40]	×4	full	32.63	0.9002	28.87	0.7889	27.77	0.7436	26.82	0.8087
SAN [9]	×4	full	32.64	0.9003	28.92	0.7888	27.78	0.7436	26.79	0.8068
IGNN [44]	×4	full	32.57	0.8998	28.85	0.7891	27.77	0.7434	26.84	0.8090
HAN [32]	×4	full	32.64	0.9002	28.90	0.7890	27.80	0.7442	26.85	0.8094
NLSA [23]	×4	full	32.59	0.9000	28.87	0.7891	27.78	0.7444	26.96	0.8109
<b>SwinIR</b> [18]	×4	full	32.72	0.9021	28.94	0.7914	27.83	0.7459	27.07	0.8164
<b>SwinIR</b> [18]	×4	50%	32.71	0.9013	28.91	0.7908	27.80	0.7466	26.91	0.8113
<b>SwinIR</b> [18]	×4	ref. 50%	32.75	0.9012	28.87	0.7903	27.81	0.7469	26.92	0.8111

the boundaries on Set14, BSD100, and Urban100 to achieve the highest metrics. Again, This indicates that a pruned dataset can match or even surpass full dataset training outcomes.

For a  $3\times$  scaling factor, the core-sets demonstrate competitive or superior performance compared to the full dataset, especially highlighted in the Set14 and BSD100 datasets. This reinforces the effectiveness of dataset pruning in enhancing model efficiency without compromising output quality significantly.

At the most challenging scaling factor of 4, the core-sets yield closely competitive results. The refined core-set offers the best PSNR on BSD100 and closely

matches the full dataset’s performance on Urban100. A general observation is that the refined core-set outperforms the original 50% core-set in most cases.

These findings underscore the potential of dataset pruning strategies, especially when applied to sophisticated models like SwinIR. The experiments suggest that thoughtful pruning can achieve comparable or superior performance using only a fraction of the training data.

## 5 Conclusion and Future Work

By introducing and comparing loss-value-based sampling strategies, our study highlights the potential of dataset pruning to maintain and, in most instances, enhance the performance of SR models while substantially reducing the computational storage. We use a simple pre-trained SR model to determine samples to remove, namely SRCNN, and apply a mean squared error loss. Our findings, particularly with the descending sampling method, underscore the value of selectively curating training datasets to include samples that are challenging for the model during training. In other words, as defined by loss values, training SR models on hard samples is more beneficial than training on easy samples. Furthermore, we evaluated that loss-value-based sampling performs better than Sobel filter-based sampling. Moreover, we showed that our refined core-set, which excludes the top 5 % of hardest samples, further improves the performance. Through several benchmarks, our approach has been validated with current state-of-the-art models. Our experiments also verify our hypothesis on several SR models, including leading models like SwinIR, and on several datasets.

For future work, we see significant potential in advancing our dataset pruning strategies by integrating more nuanced measures of sample difficulty. This could involve leveraging insights from model uncertainty or incorporating adaptive feedback loops during training to adjust the core-set dynamically. Such refinements could pave the way for more efficient training methods, optimizing computational resources while achieving superior SR model performance.

## Acknowledgements

This work was supported by the BMBF project SustainML (Grant 101070408).

## References

1. Agarwal, S., Arora, H., Anand, S., Arora, C.: Contextual diversity for active learning. In: Computer Vision—ECCV 2020: 16th European Conference, Glasgow, UK, August 23–28, 2020, Proceedings, Part XVI 16. pp. 137–153. Springer (2020)
2. Agustsson, E., Timofte, R.: Ntire 2017 challenge on single image super-resolution: Dataset and study. In: CVPRW (2017)
3. Bashir, S.M.A., Wang, Y., Khan, M., Niu, Y.: A comprehensive review of deep learning-based single image super-resolution. *PeerJ Computer Science* **7**, e621 (2021)

4. Bevilacqua, M., Roumy, A., Guillemot, C., Alberi-Morel, M.L.: Low-complexity single-image super-resolution based on nonnegative neighbor embedding (2012)
5. Cazenavette, G., Wang, T., Torralba, A., Efros, A.A., Zhu, J.Y.: Dataset distillation by matching training trajectories. In: CVPR. pp. 4750–4759 (2022)
6. Cazenavette, G., Wang, T., Torralba, A., Efros, A.A., Zhu, J.Y.: Generalizing dataset distillation via deep generative prior. In: CVPR. pp. 3739–3748 (2023)
7. Chen, X., Wang, X., Zhou, J., Qiao, Y., Dong, C.: Activating more pixels in image super-resolution transformer. In: CVPR. pp. 22367–22377 (2023)
8. Coleman, C., Yeh, C., Mussmann, S., Mirzasoleiman, B., Bailis, P., Liang, P., Leskovec, J., Zaharia, M.: Selection via proxy: Efficient data selection for deep learning. arXiv preprint arXiv:1906.11829 (2019)
9. Dai, T., Cai, J., Zhang, Y., Xia, S.T., Zhang, L.: Second-order attention network for single image super-resolution. In: CVPR. pp. 11065–11074 (2019)
10. Ding, Q., Liang, Z., Wang, L., Wang, Y., Yang, J.: Not all patches are equal: Hierarchical dataset condensation for single image super-resolution. IEEE Signal Processing Letters (2023)
11. Dong, C., Loy, C.C., He, K., Tang, X.: Image super-resolution using deep convolutional networks. IEEE TPAMI **38**(2), 295–307 (2015)
12. Dong, C., Loy, C.C., Tang, X.: Accelerating the super-resolution convolutional neural network. In: ECCV. pp. 391–407. Springer (2016)
13. Ganguli, D., Hernandez, D., Lovitt, L., Askell, A., Bai, Y., Chen, A., Conerly, T., Dassarma, N., Drain, D., Elhage, N., et al.: Predictability and surprise in large generative models. In: 2022 ACM Conference on Fairness, Accountability, and Transparency (2022)
14. Hinton, G., Vinyals, O., Dean, J.: Distilling the knowledge in a neural network. NeurIPS Workshop (2015)
15. Huang, J.B., Singh, A., Ahuja, N.: Single image super-resolution from transformed self-exemplars. In: CVPR. pp. 5197–5206 (2015)
16. Hui, Z., Wang, X., Gao, X.: Fast and accurate single image super-resolution via information distillation network. In: CVPR. pp. 723–731 (2018)
17. Katharopoulos, A., Fleuret, F.: Not all samples are created equal: Deep learning with importance sampling. In: ICML. pp. 2525–2534. PMLR (2018)
18. Liang, J., Cao, J., Sun, G., Zhang, K., Van Gool, L., Timofte, R.: Swinir: Image restoration using swin transformer. In: ICCV. pp. 1833–1844 (2021)
19. Liu, Y., Liu, A., Gu, J., Zhang, Z., Wu, W., Qiao, Y., Dong, C.: Discovering distinctive semantics in super-resolution networks. arXiv preprint arXiv:2108.00406 (2021)
20. Martin, D., Fowlkes, C., Tal, D., Malik, J.: A database of human segmented natural images and its application to evaluating segmentation algorithms and measuring ecological statistics. In: ICCV. vol. 2, pp. 416–423. IEEE (2001)
21. The Mathworks, Inc., Natick, Massachusetts: MATLAB version 9.3.0.713579 (R2017b) (2017)
22. Matsui, Y., Ito, K., Aramaki, Y., Fujimoto, A., Ogawa, T., Yamasaki, T., Aizawa, K.: Sketch-based manga retrieval using manga109 dataset. Multimedia tools and applications **76**, 21811–21838 (2017)
23. Mei, Y., Fan, Y., Zhou, Y.: Image super-resolution with non-local sparse attention. In: CVPR. pp. 3517–3526 (2021)
24. Moser, B., Frolov, S., Raue, F., Palacio, S., Dengel, A.: Waving goodbye to low-res: A diffusion-wavelet approach for image super-resolution. arXiv preprint arXiv:2304.01994 (2023)

25. Moser, B., Raue, F., Hees, J., Dengel, A.: Less is more: Proxy datasets in nas approaches. In: CVPR. pp. 1953–1961 (2022)
26. Moser, B.B., Frolov, S., Raue, F., Palacio, S., Dengel, A.: Dwa: Differential wavelet amplifier for image super-resolution. pp. 232–243. Springer (2023)
27. Moser, B.B., Frolov, S., Raue, F., Palacio, S., Dengel, A.: Yoda: You only diffuse areas. an area-masked diffusion approach for image super-resolution. arXiv preprint arXiv:2308.07977 (2023)
28. Moser, B.B., Raue, F., Frolov, S., Palacio, S., Hees, J., Dengel, A.: Hitchhiker’s guide to super-resolution: Introduction and recent advances. IEEE TPAMI (2023)
29. Moser, B.B., Raue, F., Palacio, S., Frolov, S., Dengel, A.: Latent dataset distillation with diffusion models. arXiv preprint arXiv:2403.03881 (2024)
30. Moser, B.B., Shanbhag, A.S., Raue, F., Frolov, S., Palacio, S., Dengel, A.: Diffusion models, image super-resolution and everything: A survey. arXiv preprint arXiv:2401.00736 (2024)
31. Nguyen, T., Chen, Z., Lee, J.: Dataset meta-learning from kernel ridge-regression. arXiv preprint arXiv:2011.00050 (2020)
32. Niu, B., Wen, W., Ren, W., Zhang, X., Yang, L., Wang, S., Zhang, K., Cao, X., Shen, H.: Single image super-resolution via a holistic attention network. In: ECCV. pp. 191–207. Springer (2020)
33. Paul, M., Ganguli, S., Dziugaite, G.K.: Deep learning on a data diet: Finding important examples early in training. NeurIPS **34**, 20596–20607 (2021)
34. Sener, O., Savarese, S.: Active learning for convolutional neural networks: A core-set approach. arXiv preprint arXiv:1708.00489 (2017)
35. Shleifer, S., Prokop, E.: Using small proxy datasets to accelerate hyperparameter search. arXiv preprint arXiv:1906.04887 (2019)
36. Tai, Y., Yang, J., Liu, X.: Image super-resolution via deep recursive residual network. In: CVPR. pp. 3147–3155 (2017)
37. Valsesia, D., Magli, E.: Permutation invariance and uncertainty in multitemporal image super-resolution. arXiv preprint arXiv:2105.12409 (2021)
38. Wang, T., Zhu, J.Y., Torralba, A., Efros, A.A.: Dataset distillation. arXiv preprint arXiv:1811.10959 (2018)
39. Zeyde, R., Elad, M., Protter, M.: On single image scale-up using sparse-representations. In: Curves and Surfaces: 7th International Conference, Avignon, France, June 24–30, 2010, Revised Selected Papers 7. pp. 711–730. Springer (2012)
40. Zhang, Y., Li, K., Li, K., Wang, L., Zhong, B., Fu, Y.: Image super-resolution using very deep residual channel attention networks. In: ECCV. pp. 286–301 (2018)
41. Zhang, Y., Tian, Y., Kong, Y., Zhong, B., Fu, Y.: Residual dense network for image super-resolution. In: CVPR. pp. 2472–2481 (2018)
42. Zhao, B., Bilen, H.: Synthesizing informative training samples with gan. arXiv preprint arXiv:2204.07513 (2022)
43. Zhao, B., Mopuri, K.R., Bilen, H.: Dataset condensation with gradient matching. arXiv preprint arXiv:2006.05929 (2020)
44. Zhou, S., Zhang, J., Zuo, W., Loy, C.C.: Cross-scale internal graph neural network for image super-resolution. NeurIPS **33**, 3499–3509 (2020)